MORPHOLOGIC EVOLUTION IN THE USGS SURFACE-WATER MODELING SYSTEM

Jonathan Nelson, Hydrologist, U.S. Geological Survey Geomorphology and Sediment Transport Laboratory, Golden, Colorado, jmn@usgs.gov; Richard McDonald, Hydrologist, USGS, Golden, Colorado, rmcd@usgs.gov; Paul Kinzel, Hydrologist, USGS, Golden, Colorado, pjkinzel@usgs.gov

Abstract: The morphology of an alluvial channel adjusts in response to variations in the volume and timing of water and sediment supplied to the channel. For example, hydrograph alterations due to anthropogenic causes, such as dams and diversions, produce channel adjustments over a wide variety of length and time scales; similarly, extreme flow events associated with natural variability can have profound effects on channel morphology that may produce morphologic adjustment over days to decades. For these and other important problems, geomorphologists and engineers are asked to provide quantitative assessment of the morphologic impacts of hypothetical or planned alterations in flow and/or sediment supply. Because the flow field and the morphology are intricately linked with each other and the processes of sediment transport, predicting channel form and its temporal changes in response to a known hydrograph is difficult, and better tools to address these types of problems are needed.

The USGS Multidimensional Surface Water Modeling System (MD_SWMS) was originally created as a public-domain tool for surface-water modeling in rivers and streams. The software comprises topography filtering and editing tools, grid-generation tools, two- and three-dimensional surface water models, and a wide spectrum of flexible two- and three-dimensional graphics routines for visualizing inputs to and outputs from the models. To extend MD-SWMS capabilities to providing quantitative predictions of morphologic adjustment in rivers, we incorporated routines for the prediction of sediment transport and the stepwise prediction of changes in bed elevation produced by predicted patterns of erosion and deposition. Thus, given an initial channel geometry, grain sizes making up the bed, and a hydrograph, the new version of MD_SWMS can predict the time evolution of bed morphology.

To test the approach for well-known simple geometries, we verified that MD_SWMS predicts realistic point bars in curved channels, alternate bars in straight channels with low width-to-depth ratios, and higher-mode braid bars in straight channels with higher width-to-depth ratios. The approach also predicts the formation of mid-channel bars and/or separation bars in channels with rapid expansions. A simple example of the role of discharge variations on topographic adjustment of a point bar is shown to illustrate how the new module can be used to examine such effects. We believe MD-SWMS now includes a good methodology for making quantitative predictions of channel responses to changes in flow and sediment supply and that, in the future, this and other similar approaches could be more widely used to evaluate and predict the temporal adjustment of river channels.

INTRODUCTION

The use of multidimensional flow models to predict flow in rivers and streams has increased dramatically over the past decade. This has primarily been driven by the increasingly detailed nature of the questions scientists and engineers have been trying to answer and has been facilitated by the evolution of computational power available in low-cost computers. The need for increased detail is especially clear in the areas of channel maintenance and habitat assessment in rivers; these problems are inherently tied to spatially distributed information that simple one-dimensional approaches cannot provide, so two- or three-dimensional models are required. As the application of multidimensional flow models for practical problems in rivers has become more common, the importance of considering the temporal change of erodible beds in rivers has become increasingly obvious, not just as a research goal to understand channel behavior, but as a critical part of applied problems. For example, the standard methodology in using a multidimensional model for the evaluation of channel maintenance or restoration consists of computing flows (and typically sediment transport) through a given channel form for a variety of discharges or hydrographs to evaluate the capability of the channel to carry the prescribed water and sediment discharges. Similarly, habitat assessments are generally made by taking a “snapshot” of the channel planform and bathymetry, and applying a multidimensional model for a variety of discharges in order to compute local quantities (such as velocity and depth) for comparison to some measure of habitat quality or preference. In both cases, the channel morphology is assumed to be static, whereas in reality the channel morphology will change in response to changing flow or sediment supply. Thus, for all but the simplest static channels in which morphology never changes,

predictions are strongly dependent on the actual bathymetry used for making model predictions; that bathymetry may in fact be a very poor approximation of the bathymetry for certain discharges or hydrographs. This simple point is illustrated in Figure 1, which shows two aerial photograph mosaics of a reach of the Platte River in Nebraska; the two photos were taken at similar discharges, but (a) shows the topography after a prolonged period of high flow and (b) shows the topography after a long period of low flow. Use of either set of topography for the assessment of habitat (crane roosting habitat in this case, see Kinzel et al., 2005) over a variety of discharges may yield different results, as the morphology changes dramatically depending on flow history. In this and many other similar problems, the key to improved predictions is the inclusion of temporal changes in bed morphology (i.e., morphodynamics) in multidimensional flow modeling codes.

In this paper, we present results from the new morphodynamics module recently incorporated into the U.S. Geological Survey's Multi-Dimensional Surface-Water Modeling System (MD_SWMS). The module consists of a suite of algorithms for computing local sediment transport along with a time-stepping procedure for computing the temporal evolution of the morphology of a channel bed. The components of the approach are briefly described in the sections below. To verify the behavior of the coupled models for flow, sediment transport, and bed evolution, results for the time evolution of several simple channels during a period of constant discharge also are shown below. In addition, bed evolution results for a suite of simple hydrographs for the same initial bed configuration are shown in order to exemplify how the model can be used to examine the role of real or hypothetical hydrographs in creating, maintaining, or altering channel bed morphology. In a companion paper (McDonald et al., 2006; this volume), an example of the application of the MD_SWMS morphodynamics capability for a field application is described. The new module offers a simple way to predict the temporal changes in bed morphology along with two- and three-dimensional flow patterns as required for a wide variety of practical problems.

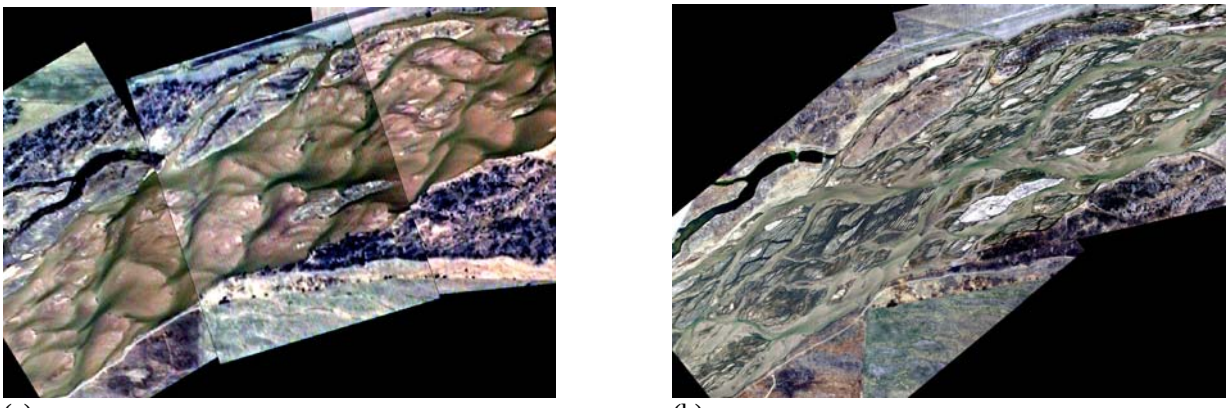

(a) (b)

Figure 1 Aerial photograph mosaic of the Platte River near Kearney Nebraska after a prolonged period of high flow (a) and a prolonged period of low flow (b). All photos taken at a discharge of approximately 1000 cfs.

THE MD_SWMS MODELING INTERFACE

The MD_SWMS modeling interface was developed by the U.S. Geological Survey as a public-domain tool for surface-water modeling in rivers and streams. The software comprises topography filtering and editing tools, grid-generation tools, two- and three-dimensional surface water models, and a wide spectrum of flexible two- and three-dimensional graphics routines for visualizing inputs to and outputs from the models. This software development program was intended to provide a means to allow both internal and public access to research models currently in use within the USGS National Research Program. MD_SWMS and its application are described in detail in the User's Guide developed by McDonald et al. (2005); the interface is available for download from the USGS at the following URL: http://wwwbrr.cr.usgs.gov/projects/SW_Env_Fluid/.

THE FASTMECH MODEL

One of the models currently available within MD-SWMS is the Flow and Sediment Transport with Mechanical Evolution of Channels (FASTMECH) model originally described in Nelson and McDonald (1996). Originally, only the flow modeling portion of the FASTMECH code was available in MD-SWMS; the module described here

incorporates the sediment transport and bed evolution components of that code with some expansion and improvements. Although the length of this paper precludes a complete description of the model development, the basic equations are given here; further details can be found in Nelson and McDonald (1996) and Nelson et al. (2003). Assuming flow is hydrostatic and incompressible and that momentum fluxes associated with vertical correlations between velocity and stress components are negligible, the vertically averaged equations of motion expressing conservation of mass and momentum in a curvilinear coordinate system with centerline radius of curvature R and streamwise and cross-stream coordinates *s* and *n* can be written as follows

$$\frac{1}{1-N}\frac{\partial}{\partial s}\left(<u>h\right)-\frac{<v>h}{(1-N)R}+\frac{\partial}{\partial n}\left(<v>h\right)=0 \tag{1}$$

$$\begin{aligned}\frac{1}{1-N}\frac{\partial}{\partial s}\left(<u>^2 h\right)+\frac{\partial}{\partial n}\left(<u><v>h\right)-\frac{2<u><v>h}{(1-N)R}=-\frac{gh}{1-N}\frac{\partial E}{\partial s}+\\ \frac{1}{\rho}\left[\frac{1}{1-N}\frac{\partial}{\partial s}\left(<\tau_{ss}>h\right)+\frac{\partial}{\partial n}\left(<\tau_{ns}>h\right)-\frac{2<\tau_{ns}>h}{(1-N)R}\right]+\\ \frac{1}{\rho}\left[\frac{1}{1-N}\left(\tau_{ss}\right)_B\frac{\partial B}{\partial s}+\left(\tau_{ns}\right)_B\frac{\partial B}{\partial n}-\left(\tau_{zs}\right)_B\right]\end{aligned} \tag{2}$$

$$\begin{aligned}\frac{1}{1-N}\frac{\partial}{\partial s}\left(<u><v>h\right)+\frac{\partial}{\partial n}\left(<v>^2 h\right)+\frac{\left(<u>^2-<v>^2\right)h}{(1-N)R}=-\frac{gh}{1-N}\frac{\partial E}{\partial n}+\\ \frac{1}{\rho}\left[\frac{1}{1-N}\frac{\partial}{\partial s}\left(<\tau_{ns}>h\right)+\frac{\partial}{\partial n}\left(<\tau_{nn}>h\right)-\frac{<\tau_{ss}-\tau_{nn}>h}{(1-N)R}\right]+\\ \frac{1}{\rho}\left[\frac{1}{1-N}\left(\tau_{ns}\right)_B\frac{\partial B}{\partial s}+\left(\tau_{nn}\right)_B\frac{\partial B}{\partial n}-\left(\tau_{zn}\right)_B\right]\end{aligned} \tag{3}$$

where < > denotes vertical averaging, *u* and *v* are the streamwise and cross-stream components of Reynolds-averaged velocity, *E* is the water surface elevation, *B* is the bed elevation, *h* is the local depth, *g* is the gravitational constant, ρ is the fluid density, $N=n/R$ and the components of the Reynolds stress tensor are given by

$$\begin{aligned}&\tau_{ss}=2\rho K\left[\frac{1}{1-N}\frac{\partial u}{\partial s}-\frac{v}{(1-N)R}\right] \qquad \tau_{nn}=2\rho K\left[\frac{\partial v}{\partial n}\right] \qquad \tau_{ns}=\rho K\left[\frac{1}{1-N}\frac{\partial v}{\partial s}+\frac{u}{(1-N)R}+\frac{\partial u}{\partial n}\right]\\ &\tau_{zn}=\rho K\left[\frac{\partial w}{\partial n}+\frac{\partial v}{\partial z}\right] \qquad \tau_{zs}=\rho K\left[\frac{1}{1-N}\frac{\partial w}{\partial s}-\frac{\partial u}{\partial z}\right] \qquad \tau_{zz}=2\rho K\left[\frac{\partial w}{\partial z}\right].\end{aligned} \tag{4}$$

In Equation 4, *K* is the value of the kinematic eddy viscosity and *w* is the vertical velocity. Because rivers are predominantly like turbulent boundary layers, *K* is set using turbulent open-channel flow results. For the solution of the vertically averaged equations above, *K* is assigned a typical vertically averaged value as follows

$$K=\frac{ku_*h}{\beta}+\alpha_H \tag{5}$$

where *k* is an empirical constant of proportionality called von Karman's constant (≈ 0.408, see Long et al. 1993), *h* is the local flow depth, β is a constant (see below), $u_*=\sqrt{\tau_B}/\rho$ and α_H is an empirical constant related to lateral diffusive processes (Nelson and McDonald, 1996)**.** The boundary shear stress, τ_B is expressed in terms of the vertically averaged velocity components using a drag coefficient closure as follows, where C_d is the drag coefficient

$$\tau_B = \rho C_d (< u >^2 + < v >^2) \,. \tag{6}$$

Splitting Equation 6 into components in the streamwise and cross-stream directions yields

$$(\tau_{zs})_B = \rho C_d \sqrt{< u >^2 + < v >^2} < u > \qquad (\tau_{zn})_B = \rho C_d \sqrt{< u >^2 + < v >^2} < v > \tag{7}$$

which allows complete closure of Equations 1 through 3. These equations are solved for the water-surface elevation and the components of vertically averaged velocity (and bed stress, through Equation 7) using the semi-implicit method for pressure linked equations (SIMPLE) presented by Patankar (1980) to iteratively solve for the water-surface elevation while solving the momentum equations for <u> and <v> using an explicit finite-difference scheme. Both schemes are used with differential relaxation to converge to a solution that satisfies the momentum equations and conserves mass both at each point and by matching the assigned discharge at each cross-section. This procedure yields the full vertically-averaged solution.

In order to develop a three-dimensional solution including the effect of secondary flows driven by channel and streamline curvature, an eddy viscosity profile is assigned along the streamlines of the vertically-averaged flow determined from the numerical solution as follows

$$K = k u_* h \kappa(\xi) \tag{8}$$

where $\kappa(\xi)$ is a shape function giving the vertical distribution of K between the bed and the water surface, using $\xi = z/h$ where h is the local flow depth and z is distance from the boundary. The choice of this function sets the value of β in Equation 5 and, along with the assumption that the vertical stress profile is approximately linear along the streamlines of the vertically averaged flow (see Nelson and Smith, 1989a), it also yields the vertical structure of the velocity along those streamlines as

$$u = u_* f(z, z_o) \tag{9}$$

where z_0, the so-called roughness length, is a constant of integration that depends on the boundary shear stress, the fluid viscosity, and/or the size of the roughness elements on the bed (see Middleton and Southard 1984, or any text on wall-bounded shear flows for a discussion of roughness lengths). Note that if $\kappa(\xi)$ is chosen to be parabolic between the bed and surface, Equation 9 is the well-known logarithmic velocity profile. In practice, slightly better results (compared to data) are found using the shape function suggested by Rattray and Mitsuda (1974), which is given by

$$\begin{aligned} \kappa(\xi) &= \xi(1-\xi) \qquad \xi < 0.2 \\ \kappa(\xi) &= 0.16 \qquad\quad \xi \geq 0.2 \end{aligned} \,. \tag{10}$$

This yields a logarithmic profile near the bed and a parabolic velocity profile in the flow interior; this shape function was used for the results shown below.

Equation 9 provides a direct relation between roughness length and the value of the boundary shear stress for a given choice of $\kappa(\xi)$. In addition, it can be used along with scaled versions of the full momentum equations to compute secondary flows perpendicular to the direction of the vertically averaged streamlines, as described by Nelson and Smith (1989b). These flows are driven by curvature of the flow streamlines and have no vertically averaged mass flux; they include the typical helical flow associated with flow in curved channels as well as the alteration in the direction of the bed stress produced by those flows. Although some aspects of this approach can at best be approximate, it does allow the computation of vertical structure and secondary flows without resorting to a full three-dimensional model, which is prohibitively slow for computing bed evolution in realistic cases.

As implemented in MD-SWMS, the FASTMECH model offers several tools for the computation of sediment flux given the solution of the flow field described above, including a variety of bedload equations, total load equations,

and advection-diffusion schemes for suspended sediment. A complete discussion of these options is outside the scope of this short paper, but all the results shown below were carried out for the case of bedload only using the so-called modified Meyer-Peter Müller equation, given by

$$(q_b)_* = 8\left[\tau_* - (\tau_*)_c\right]^{3/2} \tag{11}$$

where $(q_b)_* = \dfrac{q_b}{\left[\left(\dfrac{\rho_s - \rho}{\rho}\right) g D^3\right]^{1/2}}$, $\tau_* = \dfrac{\tau_b}{\left[(\rho_s - \rho) g D\right]}$, q_b is sediment flux per unit width in the direction of the boundary shear stress, ρ_s is sediment density, D is the sediment grain size, and $(\tau_*)_C$ is the Shields critical shear stress for sediment motion. The last component of the sediment computation algorithm is a gravitational correction to treat the effect of lateral bed slope on the direction of sediment transport. There are many such corrections, but most (e.g., those by Engelund (1974), Kikkawa et al. (1976), Hasegawa (1984) and Parker (1984)) take the form

$$q_n = q_s \left[\frac{\tau_s}{\tau_n} + \Gamma f\left(\frac{\tau_c}{\tau_b}\right)\frac{\partial B}{\partial n}\right] \tag{12}$$

where τ_s and τ_n refer to the streamwise and cross-stream components of the boundary shear stress, q_s and q_n are the streamwise and cross-stream components of bedload sediment flux, Γ is a coefficient, and f is a simple function of the ratio of critical to boundary shear stress. For details of the values of these parameters, the reader is referred to Nelson (1990). For the results here, the method of Hasegawa (1984) is used.

The final component of the bed evolution model described here is the so-called erosion equation that relates sediment flux and concentration to rates of change of the local bed elevation as follows

$$\frac{\partial B}{\partial t} = -\frac{1}{c_b}\left[\nabla \cdot \vec{q}_B + \frac{\partial}{\partial t}\int_B^E c_s dz\right] \tag{13}$$

where c_b is the concentration of sediment in the bed (taken here as 0.65) and c_s is the suspended sediment concentration. Using Equation 13 along with an assumed time step allows prediction of the evolution of channel bed topography. Thus, starting with some initial topography, the flow field is found from the numerical flow model which is, in turn, used to compute the sediment fluxes. Those values are used in Equation 13 to predict the bed morphology one time step in the future. The process is repeated iteratively to predict the temporal evolution of the bed. Time steps must be chosen such that stability is maintained, which dictates that bed changes be relatively small (typically a small fraction of the flow depth) at each time step. In practice, some experimentation with time steps is usually the best method to optimize computational time while preserving stability. For further discussion of model assumptions and limitations, the reader is referred to Nelson et al. (2003).

SIMPLE CHANNEL RESPONSE

To carry out a preliminary test of the bed evolution module that has been added to MD_SWMS, calculations were performed for a few simple channel geometries. These geometries are ones for which the basic morphological response is well known; the idea behind this simple verification was to ensure that the bed evolution model reproduced important basic responses in bed topography. There are two basic types of bar responses in rivers. First, there are bar forms that are coupled to the planform geometry of the channel such as point bars and, second, there are bar forms that arise spontaneously as a result of an instability in the coupled flow and sediment transport system, such as alternate bars. To test the model, bed evolution calculations were performed for both types of bar forms. To facilitate this, a sub-model for creating simple channels was created within MD_SWMS (the so-called "channel builder") in order to create simple initial channel forms for evolution calculations.

In Figure 2, a curved channel with initially parabolic topography is shown in plan view along with the topography predicted after 1000 minutes of bed evolution. The model predicts the formation of point bars, as expected.

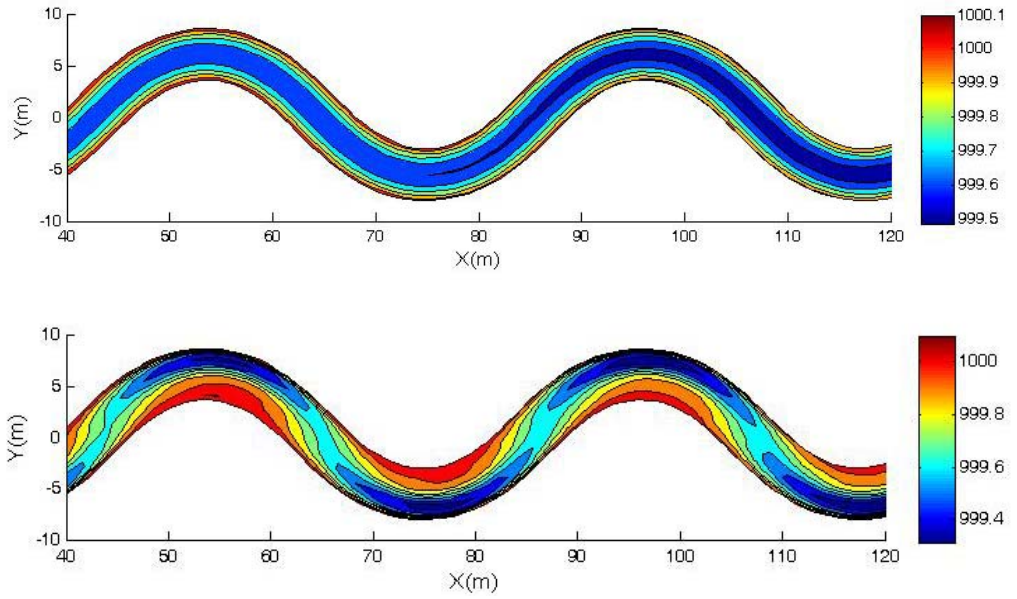

Figure 2 Initial (top) and final (bottom) topography for a simple channel described by a sine-generated curve with crossing angle of 45^o and an initially parabolic bed. The discharge is 1.0 m^3/s and the grain size is 0.5 mm.

In Figure 3, initial and final topography for a simple one-sided rectilinear channel expansion are shown. In this case, the flow in the upstream narrower channel produces much higher sediment transport in that area which is subsequently deposited downstream. Over time, the downstream deposit migrates downstream leaving a higher bed elevation so that the cross-sectional areas above and below the expansion become much more similar over time. At the same time, sediment is deposited in the eddy region, as discussed in more detail by Nelson and McDonald (1996). As in the case of the point bar, this feature is coupled to the channel planform.

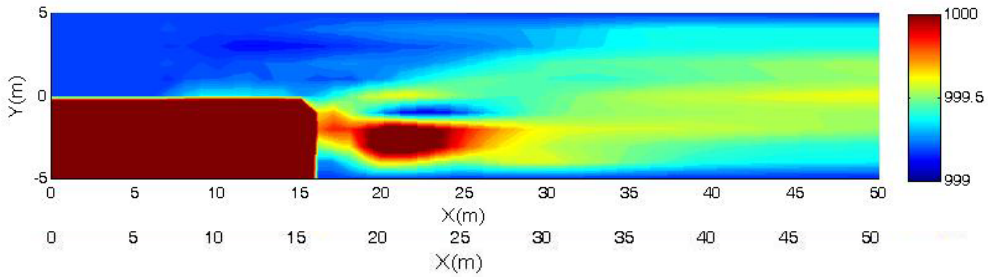

Figure 3 Initial (top) and final (bottom, after 1000 minutes) topography for a simple one-sided rectilinear expansion with discharge of 2.0 m^3/s and grain size of 0.5mm.

In Figure 4, two examples are shown for the case where planform does not force the development of bars; the bars arise from a more basic instability. In both cases, the initial channel is straight and flat-bedded, but a small

perturbation is introduced near the upstream end of the reach. This perturbation is less than 10% of the flow depth, but it is sufficient to excite the fundamental bar instability. In the upper panel, where the channel width is 20 times the depth, this results in the growth of alternate bars, but in the lower panel, where the width is 100 times the depth, a higher mode bar instability occurs, as expected.

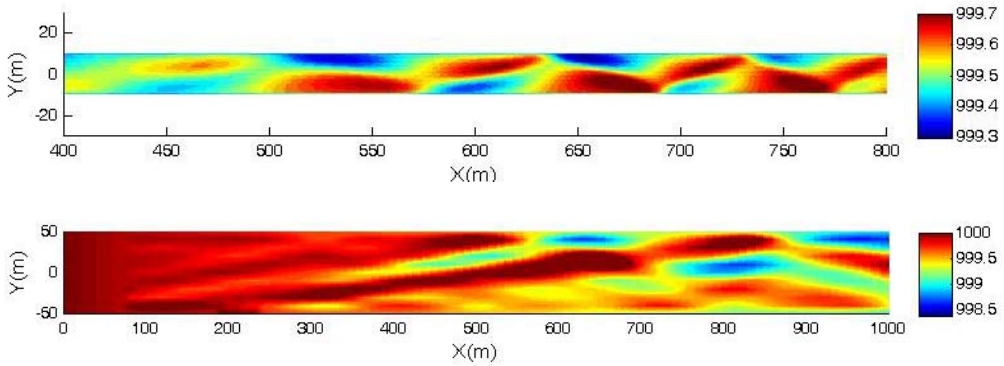

Figure 4 Topography after 1000 minutes for initially straight, flat-bedded channels with width-to-depth ratios of 20 (top) and 100 (bottom) with grain size of 0.5 mm and discharge of 5.0 and 25.0 m^3/s, respectively.

Figures 2-4 support the hypothesis that the simple bar evolution model module in MD_SWMS is capable of predicting appropriate basic behavior for well-known cases. In order to illustrate a simple case with variable discharge, channel evolution calculations were made for a simple meander (similar to that in Figure 2) for three different hydrographs, each using the same total volume of water, as shown in Figure 5.

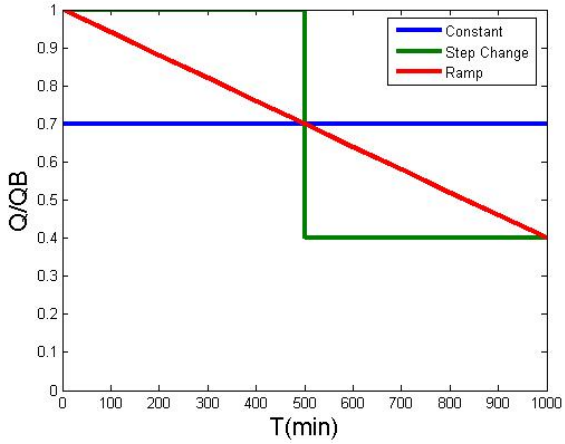

Figure 5 Three hydrographs used for examination of the effects of discharge variations on point bar growth. Q_B is the bankfull discharge for the channel.

In Figure 6, results are shown for two of the three hydrographs shown in Figure 5. As in Figure 2, the initial channel was a sine-generated planform with a parabolic bed. Note that the case where the discharge has a step change has a higher and broader point bar relative to the case where the discharge is a linear ramp. This occurs because the period of high flow allows the bar to grow higher than in the ramp case, even though the same volume of water is used. In the case with constant discharge, the bar is even smaller. This shows how the bed evolution module in MD_SWMS can be used to examine the role of hydrograph shape on resulting topography.

CONCLUSIONS

In situations where evolution of a river or stream bed is an important part of habitat or channel maintenance issues, the new bed evolution module in MD_SWMS can be used to investigate the changes in bed morphology. With further development and testing at the field scale (see McDonald et al., 2006, this volume), this new capability

expands the applicability of MD_SWMS, and allows investigation of more complex problems. Current efforts are directed at treating the formation and evolution of bedforms (ripples and dunes, see Nelson et al., 2005) and treating bank erosion and planform evolution within MD_SWMS.

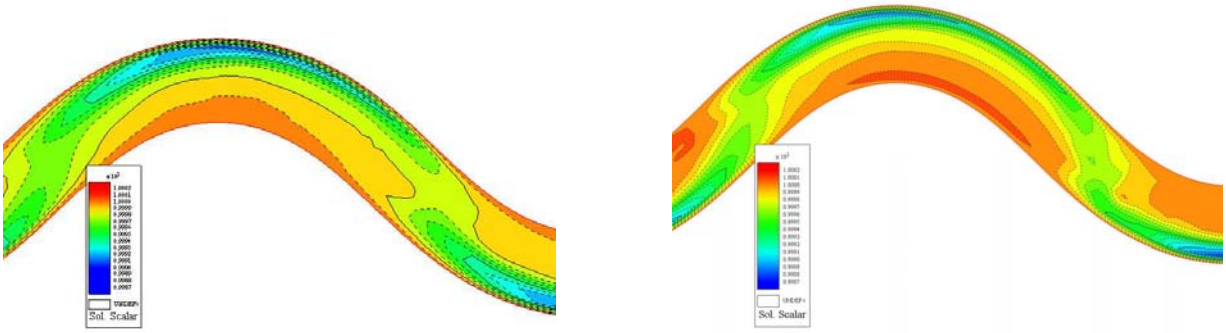

Figure 6 Bed topography in a simple meander bend after 1000 minutes of evolution using a linear ramp hydrograph (left panel) and a step hydrograph (right panel) with the same total volume.

REFERENCES

Engelund, F. (1974). "Flow and bed topography in channel bends," J. Hyd. Div. ASCE, 100(HY11): 1631-1648.

Hasegawa, K. (1984). "Hydraulic Research on Planimetric Forms, Bed Topographies, and Flow in Alluvial Channels," Ph.D. Dissertation, Hokkaido University, Sapporo, Japan.

Kikkawa, H., Ikeda, S. and Kitagawa, A. (1976). "Flow and bed topography in curved open channels," J. Hyd. Div. ASCE, 102(HY9): 1327-1342.

Kinzel, P.J., Nelson, J.M., and R.S. Parker. (2005). "Assessing sandhill crane roosting habitat along the Platte River, Nebraska," U.S. Geological Survey Factsheet 05-3029. 2p.

Long, C.E., Wiberg, P.L. and Nowell, A.R.M. (1993). "Evaluation of von Karman's constant from integral flow parameters," Journal of Hydrologic Engineering, ASCE, 119(10): 1182-1190.

McDonald, R.R., Nelson, J.M., and Bennett, J.P. (2005). "Multi-Dimensional Surface-Water Modeling System User's Guide," U.S. Geological Survey Techniques in Water Resources Investigations 11-B2, 136 p.

McDonald, R.M., Barton, G., and Nelson, J.M., in press, "Modeling hydraulic and sediment-transport processes in white sturgeon spawning habitat on the Kootenai River," Proceedings of the Federal Interagency Sedimentation Conference, this volume.

Middleton, G.V. and Southard, J.B. (1984). "Mechanics of Sediment Movement," SEPM, Tulsa. 401 pp.

Nelson, J.M., Burman, A.R., Shimizu, Y., McLean, S.R., Shreve, R.L., Schmeeckle, M.W. (2005). "Computing flow and sediment transport over bedforms," Proceedings of River Coastal and Estuarine Morphodynamics, IAHR.

Nelson, J.M., Bennett, J.P., and Wiele, S.M. (2003). "Flow and Sediment Transport Modeling," Chapter 18, p. 539-576. In: Tools in Geomorphology, eds. G.M. Kondolph and H. Piegay, Wiley and Sons, Chichester, 688 pp.

Nelson, J.M., and McDonald R.R. (1996). "Mechanics and modeling of flow and bed evolution in lateral separation eddies," Glen Canyon Environmental Studies Report, 69 pp.

Nelson, J.M. (1990). "The initial instability and finite-amplitude stability of alternate bars in straight channels," Earth-Science Reviews, 29: 97-115.

Nelson, J.M. and Smith, J.D. (1989a). "Flow in meandering channels with natural topography," In: S. Ikeda and G. Parker (eds), River Meandering, AGU Water Resources Monograph 12, Washington, D.C. 69-102.

Nelson, J.M. and Smith, J.D. (1989b). "Evolution and stability of erodible channel beds," In: S. Ikeda and G. Parker (eds), River Meandering, AGU Water Resources Monograph 12, Washington, D.C. 321-377.

Parker, G. (1984). "Discussion of: Lateral bedload transport on side slopes (by S. Ikeda, Nov., 1982)," J. Hyd. Div. ASCE, 110(2): 197-203.

Patankar, S.V. (1980). "Numerical Heat Transfer and Fluid Flow," Hemisphere, Washington, D.C. 197 pp.

Rattray, M. Jr and Mitsuda, E. (1974). "Theoretical analysis of conditions in a salt wedge," Estuarine and Coastal Marine Science, 2: 375-394